Molecular Architecture Based on Metal Triangles Derived from 2,2′-Bipyrazine (Bpz) and EnM^{II} (M = Pt, Pd)

Ralf-Dieter Schnebeck, Eva Freisinger, Frank Glahé, and Bernhard Lippert*

Contribution from Fachbereich Chemie, Universität Dortmund, D-44227 Dortmund, Germany

Received August 30, 1999

Abstract: The molecular triangle $[\{enPt(bpz\text{-}N4,N4')\}_3]^{6+}$ (en = ethylenediamine; bpz = 2,2′-bipyrazine) has been crystallized as a C_2-symmetric species (**1**), as a compound of approximate C_3 symmetry, and as a mixture of both forms (**1b**). The two triangles differ in their topologies, their Pt−Pt distances, and their anion binding properties. While for the C_2 form insertion of a single PF_6^- anion in the central cavity is seen in **1b**, the C_3 forms of **1a** and **1b** incorporate either two different anions simultaneously, NO_3^- and ClO_4^- (**1a**), or only a single PF_6^- (**1b**). Anion inclusion also occurs in solution as detected by ^1H NMR spectroscopy. The molecular triangles **1**−**1b** are the kinetic reaction products of $enPt^{II}$ and bpz. The thermodynamic product is the chelate $[enPt(bpz\text{-}N1,N1')]^{2+}$ (**2a**) that is obtained from **1** upon prolonged heating in water. The all-cis geometry of the bpz ligands in the triangle (C_3 form) can be locked by chelation of three $enPd^{II}$ to the N1,N1′ sites. Hexanuclear $[\{enPt(N4,N4'\text{-}bpz\text{-}N1,N1')Pden\}_3]^{12+}$ (**3**) has been reported by us before. Now the Pt_6 analogue **4**, the Pd_6 analogue **5**, and the isomer of **3** with the two sorts of metals inverted (**6**) have been isolated and structurally characterized. All four compounds (**3**−**6**), which crystallize as mixed NO_3^-, PF_6^- salts, have two different anions embedded in the cavity of the cations of +12 charge. Molecular triangles of the C_3 type can be fused by Ag^+ cations via N1,N1′ positions to afford the higher-nuclearity compounds Pt_6Ag_2 (**7**) and Pt_6Ag_3 (**8**). The latter encapsulates an additional Ag^+ and five NO_3^- anions in its interior (**8a**). X-ray crystal structures for **1a**, **1b**, **2a**, **4**, **5**, **6**, **7**, and **8a** are reported.

Introduction

Within the field now frequently termed "molecular architecture" efforts to utilize transition metal ions and organic ligands simultaneously have lately been particularly fruitful. As a result, a considerable variety of frequently predesigned molecular polygons and polyhedra has been established,[1−10] and a methodology exists how to combine angular and linear building blocks to generate a particular ensemble.[4−7] As far as the smallest possible polygon, the triangle, is concerned, it should be formed most readily by combining three 60° angular fragments and three linear ones (Scheme 1).[5]

However, as has correctly been noted,[5c] the number of metal-containing molecular triangles is "surprisingly small". Cyclic trinuclear metal complexes of type (A) have been prepared, among others, with heterocyclic ligands such as pyrazolate,[9] or $CH_3N{=}COCH_3$,[11] and carborane.[12] However, a triangle of type (B) with a 60° turning angle at the metal does not exist due to the impossibility of generating such an angle in a metal fragment of common coordination numbers.[13] Virtually all molecular triangles of type (B), with metal entities at the corners, display 80−90° angles.[14−25] Even a distorted tetrahedral geometry of

(1) Lehn, J.-M. *Supramolecular Chemistry: Concepts and Perspectives*; VCH: Weinheim, Germany, 1995.

(2) (a) Sauvage, J. P. *Acc. Chem. Res.* **1990**, *23*, 319. (b) Hunter, C. A. *Angew. Chem., Int. Ed. Engl.* **1995**, *34*, 1079. (c) de Mendoza, J. *Chem. Eur. J.* **1998**, *4*, 1373. (d) Navarro, J. A.; Lippert, B. *Coord. Chem. Rev.* **1999**, *185*−*186*, 653.

(3) Fyfe, M. C. T.; Stoddart, J. F. *Acc. Chem. Res.* **1997**, *30*, 393.

(4) (a) Fujita, M. J. *Synth. Org. Chem., Jpn.* **1996**, *54*, 953 and references cited therein. (b) Fujita, M. J.; Ogura, K. *Bull. Chem. Soc. Jpn.* **1996**, *69*, 1471 and references cited therein. (c) Fujita, M. J.; Ogura, K. *Coord. Chem. Rev.* **1996**, *148*, 249. (d) Takeda N.; Umemoto, K.; Yamaguchi, K.; Fujita, M. *Nature* **1999**, *398*, 794.

(5) (a) Stang, P. J.; Olenyuk, B. *Acc. Chem. Res.* **1997**, *30*, 502 and references cited therein. (b) Stang, P. J. *Chem. Eur. J.* **1998**, *4*, 19 and references cited therein. (c) Olenyuk, B.; Fechtenkötter, A.; Stang, P. J. *J. Chem. Soc., Dalton Trans.* **1998**, 1707 and references cited therein. (d) Olenyuk, B.; Witheford, J. A.; Fechtenkötter, A.; Stang, P. J. *Nature* **1999**, *398*, 796.

(6) Saalfrank, R. W.; Bernt, I.*Curr. Opin. Solid State Mater. Sci.* **1998**, *3*, 407 and references cited therein.

(7) Pecoraro, V. L.; Stemmler, A. J.; Gibney, B. R.; Bodwin, J. J.; Wang, H.; Kampf, J. W.; Barwniski, A. *Prog. Inorg. Chem.* **1997**, *45*, 83.

(8) (a) Parac, T. N.; Caulder, D. L.; Raymond, K. N. *J. Am. Chem. Soc.* **1998**, *120*, 8003. (b) Wu, H.-P.; Janiak, C.; Uehlin, L.; Klüfers, P.; Mayer, P. *Chem. Commun.* **1998**, 2637.

(9) (a) Minghetti, G.; Banditelli, G.; Bonati, F. *Inorg. Chem.* **1979**, *18*, 658. (b) Burger, W.; Strähle, J. *Z. Anorg. Allg. Chem.* **1985**, *529*, 111. (c) Raptis, R. G.; Fackler, J. P., Jr. *Inorg. Chem.* **1990**, *29*, 5003. (d) Barberá, J.; Elduque, A.; Giménez, R.; Lahoz, F. J.; Lépez, J. A.; Oro, L. A.; Serrano, J. L. *Inorg. Chem.* **1998**, *37*, 2960.

(10) (a) Farrell, J. R.; Mirkin, C. A.; Guzei, I. A.; Liable-Sands, L. A.; Rheingold, A. L. *Angew. Chem., Int. Ed. Engl.* **1998**, *37*, 465. (b) Farrell, J. R.; Mirkin, C. A.; Liable-Sands, L. A.; Rheingold, A. L. *J. Am. Chem. Soc.* **1998**, *120*, 11834.

(11) Vickery, J. C.; Balch, A. L. *Inorg. Chem.* **1997**, *36*, 5978.

(12) Zheng, Z.; Knobler, C. B.; Mortimer, M. D.; Kong, G.; Hawthorne, M. F. *Inorg. Chem.* **1996**, *35*, 1235.

(13) If high coordination numbers (≥8) are considered such a possibility exists, in principle.

(14) Chaudhuri, P.; Karpenstein, I.; Winter, M.; Butzlaff, C.; Bill, E.; Trautwein, A. X.; Flörke, U.; Haupt, H.-J. *J. Chem. Soc., Chem. Commun.* **1992**, 321.

(15) (a) McQuillan, F. S.; Berridge, T. E.; Chen, H.; Hamor, T. A.; Jones, C. J. *Inorg. Chem.* **1998**, *37*, 4959. (b) Süss-Fink, G.; Wolfender, J.-L.; Neumann, F.; Stoeckli-Evans, H. *Angew. Chem., Int. Ed. Engl.* **1990**, *29*, 429. (c) Köhler, R.; Kirmse, R.; Richter, R.; Sieler, J.; Hoyer, E.; Beyer, L. *Z. Anorg. Allg. Chem.* **1986**, *537*, 133.

(16) (a) Smith, D. P.; Baralt, E.; Morales, B.; Olmstead, M. M.; Maestre, M. F.; Fish, R. H. *J. Am. Chem. Soc.* **1992**, *114*, 10647. (b) Chen, H.; Olmstead, M. M.; Smith, D. P.; Maestre, M. F.; Fish, R. H. *Angew. Chem., Int. Ed. Engl.* **1995**, *34*, 1514.

(17) (a) Korn, S.; Sheldrick, W. S. *Inorg. Chim. Acta* **1997**, *254*, 85. (b) Schnetti, L.; Bandoli, G.; Domella, A.; Trovó, G.; Longato, B. *Inorg. Chem.* **1994**, *33*, 3169.

10.1021/ja9931325 CCC: $19.00
Published on Web 02/03/2000

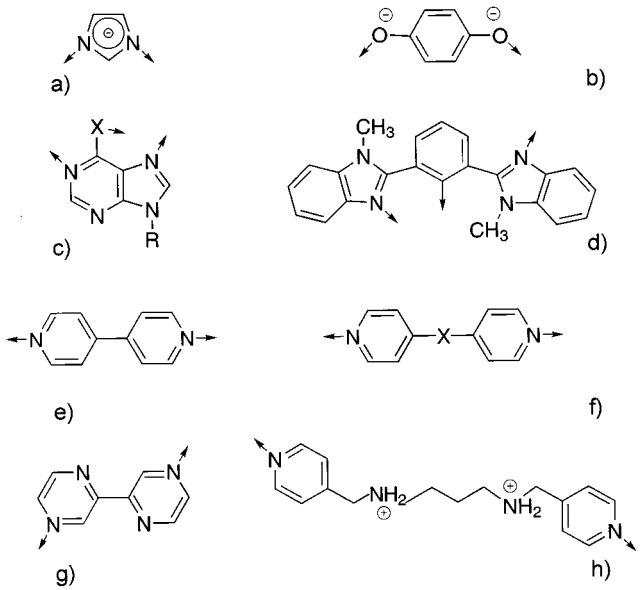

Figure 1. Selected organic ligands which enable formation of cyclic trimers with 90° metal entities at corners: (a) imidazolate,[14] (b) dianion of resorcinol,[15a] (c) 9-R-adeninate (X = NH),[16a,17] or 9-R-hypoxanthinate (X = O),[16b] (d) 1,3-bis(1-methylbenzimidazol-2-yl)benzol,[18] (e) 4,4′-bipyridine,[19] (f) X-linked 4,4′-bipyridine (X = −C≡C−, −HC=CH−, etc.),[19] (g) 2,2′-bipyrazine,[20,21] (h) *N*,*N*′-bis(4-pyridylmethyl)-1,4-diammoniumbutane.[22]

Scheme 1

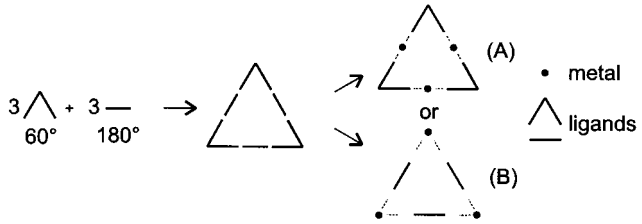

the metal, e.g., Zn^{II},[26] is possible. It is the flexibility of the organic ligand that in essence enables formation of the triangle. A few selected ligands capable of forming triangles of type (B) are illustrated in Figure 1.

The ligand we had chosen was 2,2′-bipyrazine (bpz). It undergoes rotation about the central C2−C2′ bond (5.4 kcal mol^{-1}),[27] giving rise to cis and trans conformers. Since the ring nitrogen atoms are nonprotonated over a wide pH range (pK_{a1} 0.45; pK_{a2} −1.35),[28] bpz is considered to be a rather versatile ligand (Chart 1). In addition to the established chelation mode (i) via N1 and N1′,[29] which we have confirmed,[20] we have verified also mode (ii), which leads to a molecular triangle in the case of M′ = $enPt^{II}$,[20] as well as mode (iii).[21,30] Depending on the geometry of M′, either a hexanuclear, cup-shaped species forms (M′ having a cis geometry)[21] or a flat triangle (M′ having a trans geometry).[30,31] In both cases interesting anion binding properties are observed. As will be shown in this paper, the metal binding mode (iv) likewise can produce a molecular triangle with M′ = $enPt^{II}$ which is, however, of a different topology as far as the orientation of the bridging ligands is concerned.

Chart 1

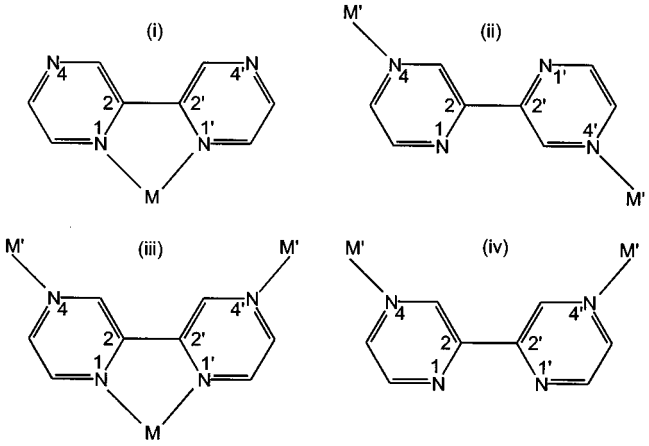

Results and Discussion

Flexibility of bpz Ligands in [{enPt(bpz-N4,N4′)}$_3$]$^{6+}$ (1). The solid-state structure of the nitrate salt of **1**, [**1**]$(NO_3)_6$,[20] had displayed trans conformations for all three bpz ligands (mode (ii) in Chart 1) and a C_2 symmetry of the cation. Inspection of the model reveals that this is just one structure (I) out of 10 possible ones (I−X), several of which are chiral (Chart 2). Formation of a hexanuclear derivate[21] with arrangement (IX) of the Pt_3 fragment had suggested that a triangle with an all-cis configuration of bpz exists in solution, which automatically implies the (transient) existence of several of the other structures in solution. Low-temperature ^{1}H NMR spectra of [**1**] $(NO_3)_6$ in DMF-d_7 reveal that below −30 °C the original three sets of resonances of the bipyrazine protons {H3(H3′), H5(H5′), and H6(H6′)} markedly broaden and lead to (at least) 10 distinguishable resonances at −55 °C. The process is fully reversible upon raising the temperature (see Supporting Information, S1, S2). From the number of resonances observed and their relative intensities at low temperature it is clear that not only the two extremes with all-trans and all-cis arrangements of the three bridging bpz ligands occur in solution. One more form (mode (iv) in Chart 1) of the molecular triangle has now been structurally characterized: In [{enPt(bpz-N4,N4′)}$_3$]$(NO_3)_2$-$(ClO_4)_4$·$2H_2O$ (**1a**) all three bpz ligands are arranged cis with respect to the C2−C2′ bonds (IX), and in [{enPt(bpz-N4,N4′)}$_3$]-$(NO_3)_2(PF_6)_4$·$3H_2O$ (**1b**), cations with an all-trans conformation (I) and an all-cis conformation (IX) of the bpz ligands crystallize

(18) Rüttimann, S.; Bernardinelli, G.; Williams, A. F. *Angew. Chem., Int. Ed. Engl.* **1993**, *32*, 392.
(19) Fujita, M.; Sasaki, O.; Mitsuhashi, T.; Fujita, T.; Yazaki, J.; Yamaguchi, K.; Ogura, K. *J. Chem. Soc., Chem. Commun.* **1996**, 1532.
(20) Schnebeck, R.-D.; Randaccio, L.; Zangrando E.; Lippert, B. *Angew. Chem., Int. Ed. Engl.* **1998**, *37*, 119.
(21) Schnebeck, R.-D.; Freisinger, E.; Lippert, B. *Angew. Chem., Int. Ed. Engl.* **1999**, *38*, 168.
(22) Whang, D.; Park, K.-M.; Heo, J.; Ashton, P.; Kim, K. *J. Am. Chem. Soc.* **1998**, *120*, 4899.
(23) Lai, S.-W.; Chan, C. C.-W.; Peng, S.-M.; Che, C.-M. *Angew., Chem. Int. Ed. Engl.* **1999**, *38*, 669.
(24) Baxter, P. N. W.; Lehn, J.-M.; Rissanen, K. *Chem. Commun.* **1997**, 1323.
(25) Baum, G.; Constable, E. C.; Fenske, D.; Housecroft, C. E.; Kulke, T.*Chem. Commun.* **1999**, 195.
(26) Thompson, A.; Rettig, S. J.; Dolphin, D. *Chem. Commun.* **1999**, 631.
(27) (a) Neto, N.; Muniz-Miranda, M.; *Spectrochem. Acta* **1994**, *50A*, 357. (b) Barone, V.; Minichino, L.; Fliszar, S.; Russo, N. *Can. J. Chem.* **1988**, *66*, 1313.
(28) Crutchley, R. J.; Kress, N.; Lever, A. B. P. *J. Am. Chem. Soc.* **1983**, *105*, 1170.
(29) Gerli, A.; Reedijk, J.; Lakin, M. T.; Spek, A. L. *Inorg. Chem.* **1995**, *34*, 1836.
(30) Schnebeck, R.-D.; Freisinger, E.; Lippert, B. *Chem. Commun.* **1999**, 675.
(31) It is noted that cis and trans refers here to geometrical isomerism about the metal M′ rather than to the ligand conformation about the C2−C2′ bond.

Chart 2

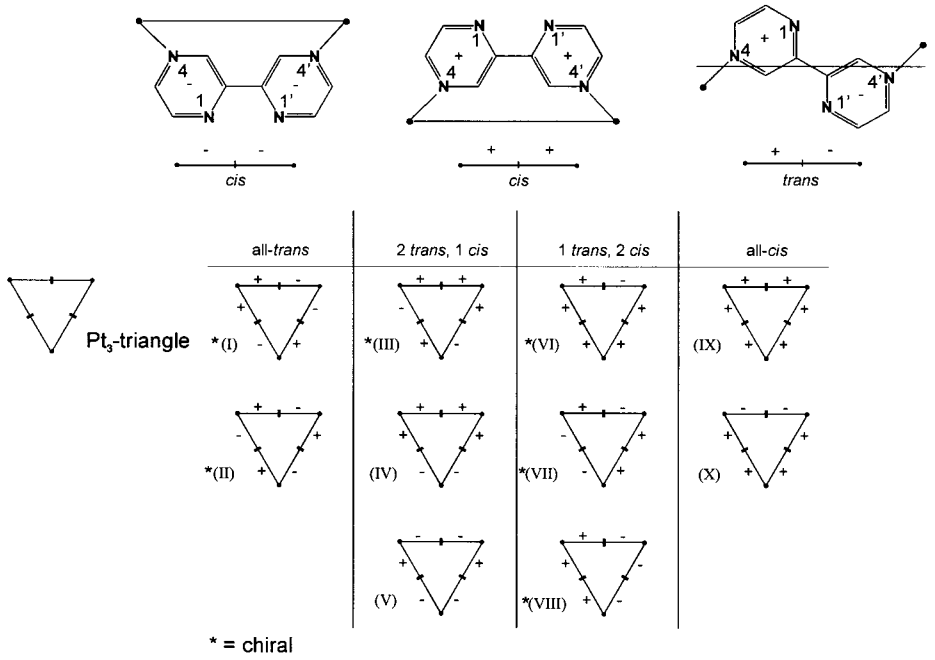

Table 1. Experimental Data for the X-ray Diffraction Studies of **1a** and **1b** and Selected Bond Lengths and Angles of **1a**, **1b**$_{(all-trans)}$, and **1b**$_{(all-cis)}$

(a) Experimental Data for **1a** and **1b**

	1a		**1b**	
formula	$C_{30}H_{44}Cl_4N_{20}O_{23}Pt_3$		$C_{60}H_{105}O_{22.5}N_{40}P_8F_{48}Pt_6$	
color, habit	redish cubes		yellowish blocks	
crystal system	triclinic		triclinic	
space group	$P\bar{1}$		$P\bar{1}$	
unit cell dimensions	$a = 12.408(2)$ Å	$\alpha = 103.19(3)°$	$a = 15.363(3)$ Å	$\alpha = 89.95(3)°$
	$b = 12.505(3)$ Å	$\beta = 91.56(3)°$	$b = 18.948(4)$ Å	$\beta = 75.24(3)°$
	$c = 17.771(4)$ Å	$\gamma = 104.95(3)°$	$c = 21.679(4)$ Å	$\gamma = 86.00(3)°$
volume (Å^3)	2582.9(9)		6086.7(21)	
Z	2		2	
formula weight (g mol^{-1})	1779.92		4077.14	
temp (K)	163(2)		123(2)	
final R indices (obs data)	$R_1 = 0.0577$	$wR_2 = 0.1423$	$R_1 = 0.0731$	$wR_2 = 0.1872$
R indices (all data)	$R_1 = 0.0875$	$wR_2 = 0.1530$	$R_1 = 0.1250$	$wR_2 = 0.2223$

(b) Bond Lengths (Å) and Angles (deg)

	1a	**1b**$_{(all-trans)}$	**1b**$_{(all-cis)}$
Pt−Pt	7.881(2)	9.279(9)	7.657(2)
	7.924(3)	9.460(3)	7.922(2)
	7.856(3)	9.542(2)	7.984(3)
N4−Pt−N4′	89.5(4)	89.1(7)	88.8(7)
	90.2(4)	89.5(6)	91.1(6)
	90.4(4)	91.2(7)	92.9(8)
torsional angles	33(2)	39(2)	24(3)
of bpz ligands	27(2)	28(2)	20(2)
	8(2)	15(2)	2(2)

side by side (Table 1a). With respect to a simplified view of the molecular all-cis triangles seen in **1a** and **1b** and a reasonable description of their hexanuclear derivatives (see below), the following procedure is helpful (Chart 3): Starting out from a fragment of a cube (i) and truncating it perpendicular to the 3-fold axis (ii), a species is generated which corresponds to the molecular triangle with the all-cis compound seen in **1a** and one of the two different cations in **1b**.

Comparison of Pt_3 Triangles (I) and (IX). In Figures 2 and 3 and Table 1b the two triangular cations are compared. There are a number of major structural differences between the all-trans structures of **1** and **1b**, as well as the all-cis structures in **1a** and the second cation in **1b**: First, the overall shape of the two triangles and their dimensions are different. The all-trans compound provides the impression of a triangle more clearly than the all-cis compound, which looks more like a vase or a double cone, if the en ligands are considered. Second, Pt−Pt distances are significantly shorter in the all-cis structure (ca. 7.7−8.0 Å) than in the all-trans structures (ca. 9.4 Å). This is a consequence of the relative orientations of N4 and N4′ in the two rotamers (Chart 1, (ii) and (iv)). Third, the two halves of bpz in the all-trans structures are markedly twisted (torsional angles ca. 15−39°) whereas in the all-cis structures one bpz ligand is roughly planar (ca. 2°, 8°) while the other two are more strongly twisted (ca. 20−33°). Fourth, angles between Pt_3 planes and the bpz ligands are in the all-trans compound nearly

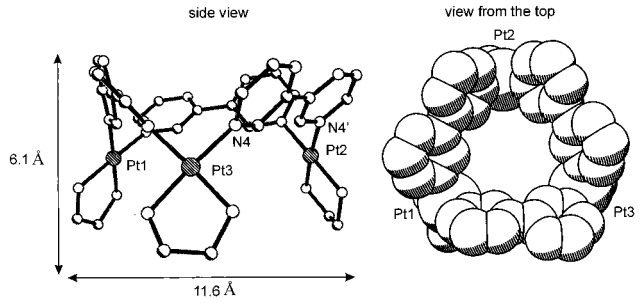

Figure 2. Views and dimensions of the cation of **1a** with all-cis conformations of the 2,2′-bpz ligands. Given dimensions refer to distances between C atoms, not protons.

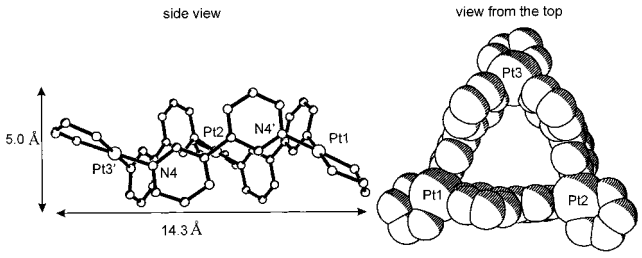

Figure 3. Views and dimensions of the cation with all-trans conformations of bpz in **1b**. Given dimensions refer to distances between C atoms, not protons.

Chart 3

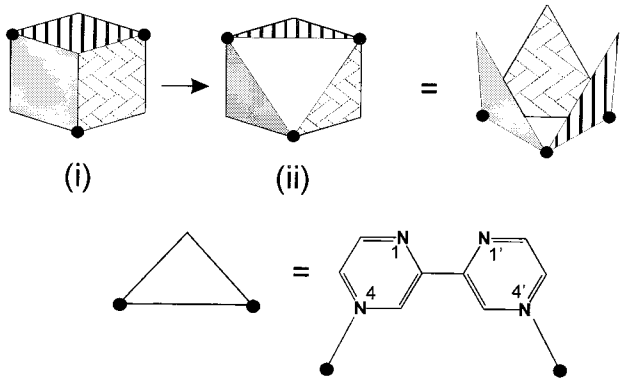

90° and in the all-cis configuration between 130° and 135°. Fifth, anions interact differently with the two rotamers (see below).

Anion Binding of 1a and 1b in the Solid-State and in Solution. There are remarkable differences in the solid state structures of the two molecular Pt triangles of bpz as far as interactions with anions are concerned. These findings may indeed be indicative of an important role of cation−anion contacts in stabilizing or even inducing a particular rotamer structure. The previously described all-trans rotamer **1** had been crystallized as the nitrate salt.[20] No anion was located in the cavity of the triangle. However, the all-trans rotamer of the mixed NO_3^-, PF_6^- salt **1b** displays a PF_6^- anion within the triangular cavity (Figure 4a). PF_6^- is also inserted in the cavity of the all-cis rotamer in the very same compound **1b** (Figure 4b). There exist distinct differences in the way the PF_6^- anions are included in the cavities of the two rotamers. In the all-trans species a face of the octahedral PF_6^- anion points toward the three Pt atoms, giving rise to long Pt−F distances (4.13(2)−4.98(2) Å), with P approximately 2.6 Å above the Pt_3 plane. In contrast, in the all-cis species a single F ligand of PF_6^- points toward the Pt_3 plane (Pt_3···F 2.23(2) Å; Pt_3···P 3.64(1) Å) while four equatorial F ligands of PF_6^- are directed toward the bpz

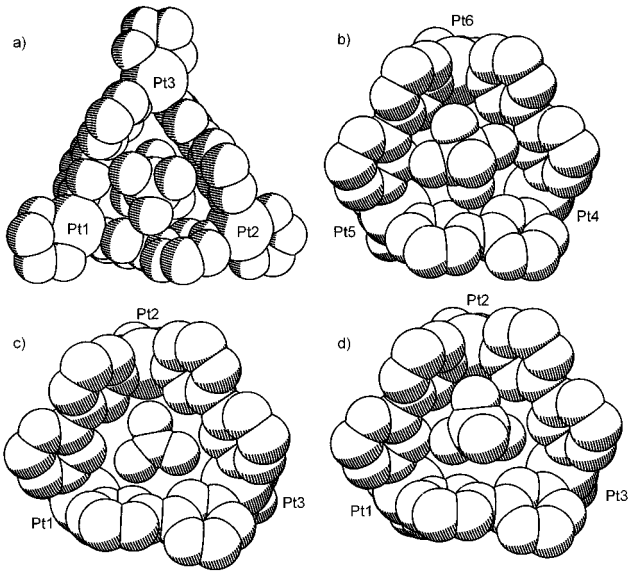

Figure 4. Space filling representations of cation−anion interactions: (a) all-trans conformer of **1b** with PF_6^- inserted into the cavity; (b) all-cis conformer of **1b** with PF_6^-; (c) all-cis conformer **1a** with NO_3^-; and (d) all-cis conformer **1a** with ClO_4^-. In parts c and d both anions are bound simultaneously, but for clarity the respective other anion is omitted. Note the different orientations of PF_6^- anions in parts a and b.

ligands. Distances between F and the heteroaromatic C protons are 2.77(3)−3.23(4) Å, suggesting some very weak CH···F hydrogen bonding. The crucial role of PF_6^- in supramolecular organization processes and anion-assisted self-assembly has been pointed out by Stoddart in a series of papers.[32] As in these cases, the PF_6^- anions incorporated in our Pt_3 triangles are not disordered, strongly suggesting a structural role of these anions that goes beyond their functions as counterions for charge neutralization.

The all-cis compound **1a**, which was crystallized as a mixed NO_3^-, ClO_4^- salt, shows both anions bound in the cavity of the trinuclear cation in the solid state. The NO_3^- ion is lying approximately in the Pt_3 plane (Figure 4c), with oxygen atoms pointing toward the Lewis acidic Pt centers (Pt···O 3.2(1)−3.5(1) Å). The ClO_4^- anion is on top of the NO_3^- ion, with Cl located approximately 3.5 Å above the Pt_3 plane (Figure 4d). Although not in an ideal fashion, the O_3 face of the ClO_4^- ion points toward the three Pt atoms (ca. 4.3−4.8 Å). This situation is reminiscent of the situation in the previously described hexanuclear Pt_3Pd_3 compound of the all-cis rotamer.[21]

In summary, the all-cis triangle behaves as a versatile host for anions, incorporating trigonal-planar NO_3^-, tetrahedral ClO_4^-, and octahedral PF_6^-, and even combining the first two anions. Apparently the longer Pt−Pt separations (ca. 9.4 Å) in the all-trans rotamer are not particularly favorable for inclusion of NO_3^- as in the case of the all-cis rotamer. Nevertheless, NO_3^- by itself seems not to be capable of forcing the Pt_3 triangle to adopt an all-cis arrangement, as evident from the crystal structure of **1**, but a combination of NO_3^- and tetrahedral ClO_4^- apparently stabilizes this form.

(32) Ashton, P. R.; Fyfe, M. C. T.; Glink, P. T.; Menzer, S.; Stoddart, J. F.; White, A. J. P.; Williams, D. J. *J. Am. Chem. Soc*. **1997**, *119*, 12514. (b) Fyfe, M. C. T.; Glink, P. T.; Menzer, S.; Stoddart, J. F.; White, A. J. P.; Williams, D. J. *Angew. Chem., Int. Ed. Engl*. **1997**, *36*, 2068. (c) Ashton, P. R.; Fyfe, M. C. T.; Martinez-Diaz, M.-V.; Menzer, S.; Schiavo, C.; Stoddart, J. F.; White, A. J. P.; Williams, D. J. *Chem. Eur. J*. **1998**, *4*, 1523. (d) Ashton, P. R.; Fyfe, M. C. T.; Hickingbottom, S. K.; Menzer, S.; Stoddart, J. F.; White, A. J. P.; Williams, D. J. *Chem. Eur. J*. **1998**, *4*, 577.

Table 2. Association Constants (K_{ass} [M^{-1}] $\pm$ 3σ) for Anion Binding by **1** and **3***

	1	**3*** [a]
PF_6^-	13.5 $\pm$ 3.1	10.6 $\pm$ 3.9
ClO_4^-	32.8 $\pm$ 7.7	9.6 $\pm$ 4.5
BF_4^-	42.1 $\pm$ 11.7	4.1 $\pm$ 1.1
SO_4^{2-}	24 $\pm$ 7.9	255.8 $\pm$ 57.3

[a] **3*** pure nitrate compound of **3** (ref 21)

Chart 4

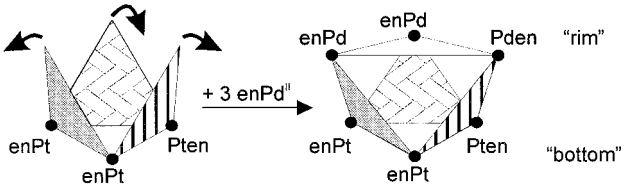

^{1}H NMR spectroscopy has been applied to study anion−cation interactions of **1**. To solutions of the NO_3^- salt **1** increasing amounts of NH_4PF_6, $NaClO_4$, $NaBF_4$, and Na_2SO_4 had been added and the changes in chemical shifts of the aromatic protons had been monitored (Supporting Information S3). In all cases averaged signals are observed only, meaning that rigid structures of the individual rotamers are not formed. The presence of PF_6^-, ClO_4^-, and BF_4^- causes a smooth highfield shift of the H3(H3′) resonances of the bpz ligands ($\Delta\delta$ ClO_4^-, 0.05 ppm; PF_6^-, 0.15 ppm; BF_4^-, 0.03 ppm; 10 equiv of salt each) and in the case of PF_6^- an additional slight downfield shift (Δ δ 0.01 ppm) of H5(H5′). In contrast, SO_4^{2-} causes shifts H5(H5′) downfield by 0.05 ppm (10 equiv of salt). From these shifts, association constants have been determined (Table 2). Not unexpectedly, the absolute values are not particularly large as a consequence of the use of the polar solvent water. The data do not permit detailed conclusions concerning the effect of these anions on the rotamer distribution.

Conversion of Triangle 1 to Chelate 2a. $[enPd(H_2O)_2]^{2+}$ reacts with bpz not to the triangular analogues of **1**, **1a**, and **1b**, but rather to the mononuclear species $[enPd(bpz\text{-}N1,N1')]^{2+}$ (**2**).[20] This finding had suggested that a mononuclear chelate complex with N1,N1′ metal binding is the thermodynamically favored product, and that the triangular species derived from $enPt^{II}$ are the kinetically favored ones. Indeed, heating (100 °C) **1** in water for a prolonged period of time (14 d) leads to a smooth and quantitative interconversion of **1** → 3·**2a** (Supporting Information). $[enPt(bpz\text{-}N1,N1')](NO_3)_2$ (**2a**) was characterized by X-ray crystallography (Supporting Information). Structural details of **2a** are very similar to those of the analogous Pd compound **2**.[20] The ^{1}H NMR signal pattern of **2** resembles that of the analogous Pd chelate,[20] and the ^{195}Pt NMR resonance (−2749 ppm, D_2O) is consistent with a PtN_4 coordination sphere.

Hexanuclear Vases. As pointed out above, the all-cis structure of the Pt_3 triangle can be locked by chelating three $enPd^{II}$ moieties via the N1 and N1′ positions. The resulting hexanuclear structure,[21] $[\{enPt(N4,N4'\text{-}bpz\text{-}N1,N1')Pden\}_3]^{12+}$ (**3**), can be described as a cup or a flat vase with an equilateral Pt triangle at the bottom (Pt−Pt, ca. 7.9 Å each) and an almost isosceles Pd_3 triangle at the rim (Pd−Pd, ca. 8.4, 8.6, 9.7 Å) and nearest Pt−Pd separations of ca. 6.8 Å. Thus, compared to the ideal situation depicted in Chart 3, in **3** the trigonal antiprism is somewhat compressed and slightly irregular (Chart 4). Applying two different synthetic routes we have now prepared also the linkage isomer of **3**, with the three metal triangles inverted (**6**), and in addition the corresponding Pt_6 (**4**) and Pd_6 (**5**) vases.

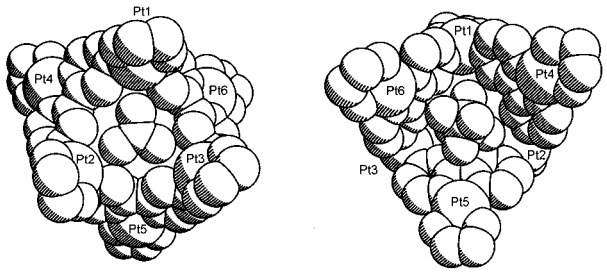

Figure 5. Space filling representations of Pt_6 complex **4** with simultaneous incorporation of NO_3^- and PF_6^-. The NO_3^- is viewed from the bottom of the cation (plane of Pt1, Pt2, Pt3 closest to viewer), whereas the PF_6^- is viewed from the top (Pt4, Pt5, Pt6 triangle closest to viewer).

$[\{enPt(N4,N4'\text{-}bpz\text{-}N1,N1')Pten\}_3](NO_3)_7(PF_6)_5\cdot 4H_2O$ (**4**) has been prepared in analogy to **3**, starting from the Pt_3 triangle **1** and adding an excess of $[enPt(H_2O)_2]^{2+}$ and suitable counteranions for crystallization. In contrast, $[\{enPd(N4,N4'\text{-}bpz\text{-}N1,N1')Pden\}_3](NO_3)_4(PF_6)_8\cdot 5H_2O$ (**5**) has been obtained from mononuclear **2** in the presence of an excess of $[enPd(H_2O)_2]^{2+}$ according to:

$$3[enPd(bpz\text{-}N1,N1')]^{2+} + 3[enPd(H_2O)_2]^{2+} \rightarrow \mathbf{5}$$

Similarly, $[\{enPd(N4,N4'\text{-}bpz\text{-}N1,N1')Pten\}_3](NO_3)_7(PF_6)_5\cdot 9.75H_2O$ (**6**) was prepared from mononuclear **2a** and an excess of $[enPd(H_2O)_2]^{2+}$. The cations of **4**−**6** are depicted in the Supporting Information (S6−S8). They have a close structural analogy with **3**.[21] A comparison of salient structural features of all four compounds is given in Tables 3, parts a and b.

The addition of three enM^{II} entities to the rim of the all-cis rotamer substantially enlarges the central cavity and increases the charge of the cation from +6 to +12. All four complexes **3**−**6** were crystallized as mixed NO_3^-, PF_6^- salts and display a rather similar anion binding pattern,[21] with a nitrate anion in the bottom M_3 plane and a hexafluorophosphate anion on top (Figure 5, compound **4**). The remaining 10 anions form multiple H bonding interactions with the cation and the water molecules.

We have previously reported association constants between the mixed Pt_3Pd_3 complex **3** and different anions in water.[21] Due to the instability of **4**−**6** in solution (see below), analogous measurements have not been performed with these compounds.

NMR Spectra. Selected ^{1}H NMR spectra (D_2O, aromatic region only) of the compounds described in this paper are provided in the Supporting Information (S9). The interpretation of the spectrum of the Pt chelate **2a** is straightforward. The singlet at 9.80 ppm is attributed to H3(H3′), and the doublets at 9.08 and 8.89 ppm ($^3J_{5,6}$ = 3.5 Hz) to H5(H5′) and H6(H6′), respectively. Differentiation of the latter two protons is made by differences in ^{195}Pt coupling (40.0 Hz with H6(H6′)).

The aromatic bpz protons of the Pt_3 compound **1** consist of a singlet for H3(H3′) at 9.33 ppm, a doublet at 9.10 ($^3J_{5,6}$ = 3.2 Hz), and a doublet of doublets at 8.84 ppm ($^5J_{3,6}$ = 1.1 Hz, $^3J_{5,6}$ = 3.2 Hz) for H5(H5′) and H6(H6′), respectively. A resonance at −2753 ppm in the ^{195}Pt NMR spectrum confirms PtN_4 coordination. In DMF-d_7 (ambient temperature) all three protons of **1** occur as broadened singlets at somewhat different chemical shifts (H3,(H3′), s 9.39 ppm; H5,(H5′), d 9.41 ppm, $^3J_{5,6}$ = 2.9 Hz; H6,(H6′), d 8.96 ppm).

The Pt_6 compound **4** has the H3(H3′) singlet at 10.56 ppm and two doublets at 9.80 and 9.26 ppm ($^3J_{5,6}$ 3.9 Hz), assigned

Table 3. Experimental Data for the X-ray Diffraction Study of **4**, **5**, and **6** and Selected Bond Lengths and Angles for **3**, **4**, **5**, and **6**

(a) Experimental Data for **4**, **5**, and **6**

	4	5	6
empirical formula	$C_{36}H_{74}O_{25}N_{31}P_5F_{30}Pt_6$	$C_{36}H_{76}O_{17}N_{28}P_8F_{48}Pd_6$	$C_{36}H_{85.5}O_{30.75}N_{31}P_5F_{30}Pd_3Pt_3$
color, habit	yellow cubes	yellow-green cubes	yellow-brown cubes
crystal system	monoclinic	monoclinic	monoclinic
space group	$P2_1/c$	$P2_1/c$	$P2_1/c$
unit cell dimens	$a = 16.992(3)$ Å	$a = 16.977(3)$ Å	$a = 16.920(3)$ Å
	$b = 23.817(5)$ Å, $\beta = 95.19(3)°$	$b = 22.705(5)$ Å, $\beta = 93.74(3)°$	$b = 24.099(5)$ Å, $\beta = 95.18(3)°$
	$c = 21.944(4)$ Å	$c = 22.737(5)$ Å	$c = 22.146(4)$ Å
volume (Å^3)	8844.3(31)	8844.4(31)	8993.3(31)
Z	4	4	4
formula wt (g mol^{-1})	3236.65	2971.41	3074.17
temp (K)	126(2)	133(1)	143(2)
final *R* indices (obs data)	$R_1 = 0.0774$; $wR_2 = 0.2063$	$R_1 = 0.0506$; $wR_2 = 0.1115$	$R_1 = 0.0937$; $wR_2 = 0.2266$
R indices (all data)	$R_1 = 0.1168$; $wR_2 = 0.2338$	$R_1 = 0.1095$; $wR_2 = 0.1341$	$R_1 = 0.1161$; $wR_2 = 0.2583$
goodness-of-fit (obs data)	1.224	1.119	1.209

(b) Bond Lengths (Å) and Angles (deg)

	3[a]	**4**	**5**
($M_{N4,N4'}-M_{N4,N4'}$)[b]	7.85(1)	7.85(1)	7.85(1)
	7.87(1)	7.85(1)	7.88(1)
	7.90(1)	7.88(1)	7.89(1)
($M_{N1,N1'}-M_{N1,N1'}$)[c]	8.39(1)	9.12(1)	8.32(1)
	8.55(1)	9.86(1)	8.55(1)
	9.77(1)	10.05(1)	9.79(1)
N4−M−N4′	87.3(3)	88(2)	87.4(3)
	87.4(3)	91(2)	87.6(3)
	89.1(3)	92(2)	89.3(3)
N1−M−N1′	80.7(3)	81(2)	80.6(3)
	80.8(3)	81(2)	80.9(3)
	81.2(3)	82(3)	80.9(3)
$M_{N1}-ONO_2$	3.21(1)	3.26(4)	3.22(1)
	3.39(1)	3.29(4)	3.41(1)
	3.49(1)	3.43(5)	3.48(1)
$M_{N1}-FPF_5$	3.39(1)	3.97(6)	3.36(1)
	3.88(1)	3.99(8)	3.87(1)
	4.31(1)	5.15(9)	4.31(1)
$M_{N4}-FPF_5$	3.87(1)	4.18(5)	3.86(1)
	4.61(1)	4.27(9)	4.45(1)
	4.42(1)	4.61(8)	4.56(1)

[a] Data taken from ref 21. [b] M−M distances of metal ions coordinated via the N4, N4′ sites of bpz. [c] M−M distances of metal ions coordinated via the N1, N1′ sites of bpz.

to H5(H5′) and H6(H6′). As expected from binding of two metal entities to bpz via N1,N1′ and N4,N4′, the chemical shifts of the aromatic protons of **4** are furthest downfield with respect to those of **2a** and **1**. The ^{195}Pt NMR spectrum shows two resonances of 1:1 intensities at −2704 and −2715 ppm, indicative of the two types of Pt atoms with a PtN_4 environment each. Surprisingly **4** appears not to be particularly stable in solution, unlike the mixed Pt_3Pd_3 compound **3**.

The Pd_6 species **5** and the mixed Pd_3Pt_3 compound **6** are essentially fully dissociated in solution. The ^{1}H NMR spectrum in D_2O of **5** indicates the presence of $[enPd(bpz\text{-}N1,N1')]^{2+}$ and $[enPd(D_2O)_2]^{2+}$, and the solution spectrum of **6** displays resonances of the building blocks, $[enPt(bpz\text{-}N1,N1']^{2+}$ (**2a**) and $[enPd(D_2O)_2]^{2+}$ only.

Linking Pt_3 Triangles via Ag^+. Previous reports on polymeric Ag^+ complexes of pyrazine[33] prompted us to also study reactions of the triangle **1** with Ag^+. Of the isolated compounds, two representative examples of molecular species will be discussed in the following. Formation of the octanuclear compound $[\{enPt(bpz\text{-}N4,N4')\}_3AgNO_3]_2(NO_3)_8(PF_6)_4\cdot 15.5H_2O$ (**7**) and of the decanuclear compound $[\{enPt(bpz\text{-}N4,N4')\}_3(AgNO_3)_{1.5}]_2(NO_3)_{12}\cdot AgNO_3\cdot 22H_2O$ (**8a**) are sketched in Chart 5.

The centrosymmetric cation of **7** is depicted in Figure 6a. As can be seen, all bpz rings are in cis configurations, but only two of the three bpz rings of a Pt_3 triangle interact with Ag. The Ag^+ ions adopt highly distorted octahedral *cis*-$(N1,N1')_2O_2$ coordination geometries, with the two oxygen donors coming from chelating nitrate anions. Angles about the Ag vary between 47(2) and 147(2)°. Selected structural features are listed in Table 4, parts a and b. Figure 6b gives a detailed structure, namely the central heteronuclear metallomacrocycle, which is an almost ideal molecular square with intermetallic distances of ca. 7.2 Å and angles close to 90°. The bpz ligands interconnecting the four metal ions are essentially perpendicular to the square, unlike in many other molecular squares[4,5] where some of the ligands are substantially tilted. In a way, **7** can thus be described as a heterometallic square spanned by two Pt_2 containing handles. A remarkable feature of **7** is again its propensity to bind PF_6^- anions in the two cavities provided by the bpz ligands in the cis conformation (Chart 5, top, and Figure 7). Although **7** crystallizes as a mixed NO_3^-, PF_6^- salt, nitrate is not binding to the Pt_3 plane. Rather the PF_6^- is in an arrangement similar to that found with the all-cis rotamer in **1b** (cf. Figure 4b). P is 3.74(2) Å above the Pt_3 plane.

(33) (a) Carlucci, L.; Ciani, G.; Proserpio, D. M.; Sironi, A. *Angew. Chem., Int. Ed. Engl.* **1995**, *34*, 1895. (b) Carlucci, L.; Ciani, G.; Proserpio, D. M.; Sironi, A. *Inorg. Chem.* **1995**, *34*, 5698. (c) Carlucci, L.; Ciani, G.; Proserpio, D. M.; Sironi, A. *J. Am. Chem. Soc.* **1995**, *117*, 4562.

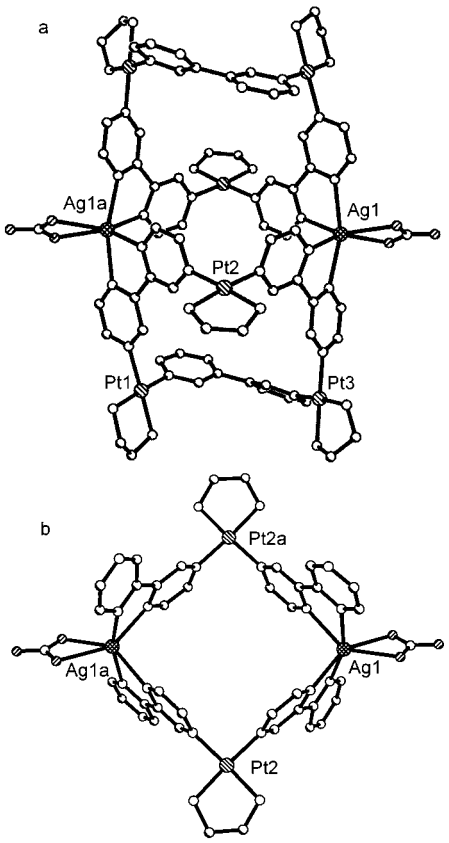

Figure 6. X-ray crystal structure of (a) cation **7** and (b) detail of the central molecular Pt_2Ag_2 square.

Chart 5

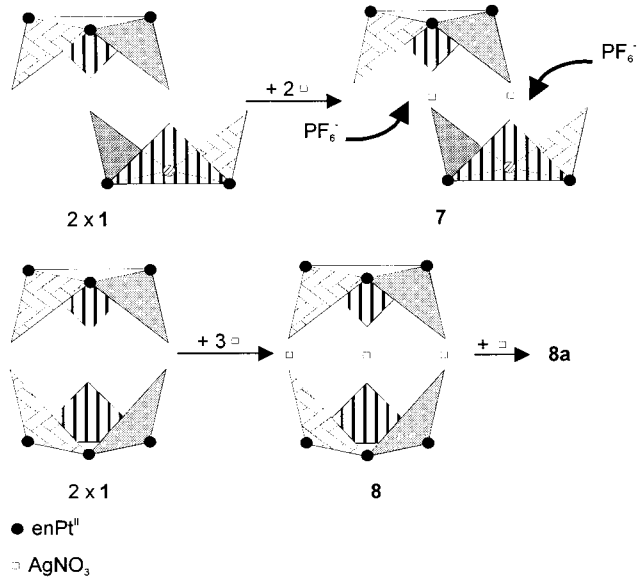

In Figure 8 two views of the spherical cation **8a** are given. It is composed of two Pt_3 cups of **1** (with bpz in the all-cis conformation) which are connected via three $AgNO_3$ units on a mirror plane, and an additional Ag^+ located within the central cavity. As with **7**, the Ag^+ ions interconnecting the Pt triangles are bound to two pairs of N1,N1′ nitrogen atoms of a bpz ligand and to two oxygen atoms of a chelating or, taking into account the asymmetry of NO_3^- binding, semichelating nitrate anion. The overall shape of the cation **8** is that of a barrel, the interior of which can be accessed from either end (at Pt_3 planes), but is otherwise almost closed (Figure 8, bottom). The analogy between **8** and an organic carcerand[34] is obvious and although restricted to the solid state, also the analogy between **8a** and a carceplex is justified.

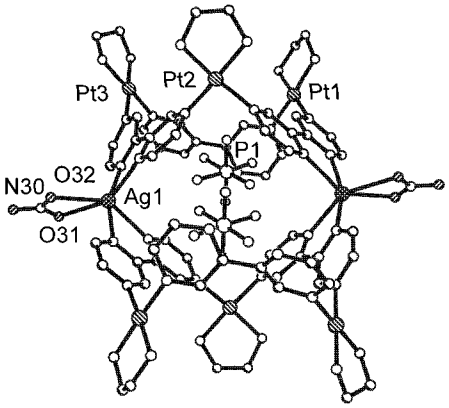

Figure 7. Encapsulation of two PF_6^- anions in the cavities of **7**. The lower Pt-triangle is facing the viewer, while the upper one extends behind the plane of the paper.

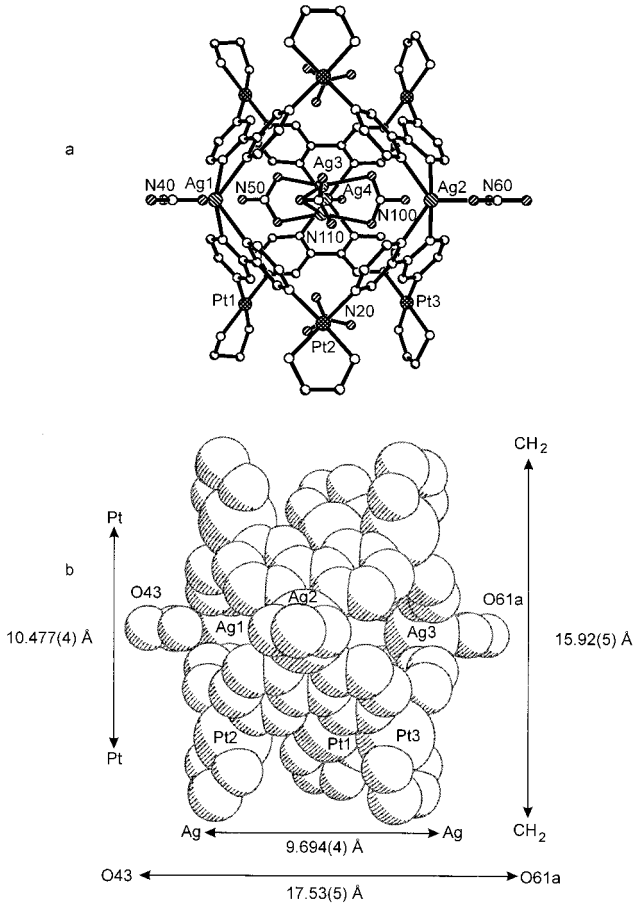

Figure 8. (a) Molecular container **8a**, consisting of Pt_6Ag_3 framework **8** and incorporated Ag^+ (disordered Ag(4)) as well as NO_3^- anions (N50, N100, N110 in the central cavity; N20 at the bottom and the top of the container). (b) Space filling representation (side view) and dimensions of **8**. In the solid state, the nitrate anion bound to Ag(2) bridges to Ag(3) of a symmetry related cation (x+1,y,z), thereby generating an infinite string of cations.

Salient crystallographic data of **8a** are provided in Table 5, parts a and b. The Pt_3 triangles are close to equilateral (7.77 Å, av). The triangle formed by the three outer Ag^+ ions is also

(34) (a) Cram, D. J. *Angew. Chem., Int. Ed. Engl.* **1988**, *27*, 1009. (b) Cram, D. J. *Nature* **1992**, *356*, 29. (c) Jasat, A.; Sherman, J. C. *Chem. Rev.* **1999**, *99*, 931.

Table 4. Experimental Data for the X-ray Diffraction Study of **7** and Selected Bond Length and Angles of **7**

(a) Experimental Data

formula	$C_{60}H_{115}O_{45.5}N_{46}P_4F_{24}Pt_6Ag_2$	volume (Å^3)	6171.7(22)
color, habit	yellow cubes	Z	2
crystal system	monoclinic	formula wt (g mol^{-1})	4175.14
Space group	*P*2/*c*	temp (K)	114(2)
unit cell dimens	$a = 14.936(3)$ Å	final *R* indices (obs data)	$R_1 = 0.0528$; $wR_2 = 0.1276$
	$b = 13.216(3)$ Å, $\beta = 95.43(3)$	*R* indices (all data)	$R_1 = 0.1058$; $wR_2 = 0.1702$
	$c = 31.407(6)$ Å	goodness-of-fit (obs data)	1.121

(b) Bond Lengths (Å) and Angles (deg) of **7**

Pt(1)−N(41)	2.01(4)	N(41)−Pt(1)−N(4′3)	89(2)
Pt(1)−N(4′3)	2.03(4)	N(41)−Pt(1)−N(11P)	94(2)
Pt(1)−N(11P)	2.04(4)	N(4′3)−Pt(1)−N(11P)	176(2)
Pt(1)−N(12P)	2.05(4)	N(41)−Pt(1)−N(12P)	177(2)
Pt(2)−N(22P)	2.02(5)	N(4′3)−Pt(1)−N(12P)	94(2)
Pt(2)−N(4′1)	2.02(5)	N(11P)−Pt(1)−N(12P)	83(2)
Pt(2)−N(42)	2.02(4)	N(22P)−Pt(2)−N(4′1)	176(2)
Pt(2)−N(21P)	2.05(4)	N(22P)−Pt(2)−N(42)	92(2)
Pt(3)−N(4′2)	1.99(4)	N(4′1)−Pt(2)−N(42)	92(2)
Pt(3)−N(31P)	2.00(5)	N(22P)−Pt(2)−N(21P)	85(2)
Pt(3)−N(32P)	2.01(5)	N(4′1)−Pt(2)−N(21P)	91(2)
Pt(3)−N(43)	2.01(5)	N(42)−Pt(2)−N(21P)	177(2)
Ag(1)−N(11)[a]	2.38(5)	N(4′2)−Pt(3)−N(31P)	178(2)
Ag(1)−N(1′2)	2.40(5)	N(4′2)−Pt(3)−N(32P)	94(2)
Ag(1)−N(12)	2.42(4)	N(31P)−Pt(3)−N(32P)	84(3)
Ag(1)−N(1′1)[a]	2.46(5)	N(4′2)−Pt(3)−N(43)	88(2)
Ag(1)−O(32)	2.50(5)	N(31P)−Pt(3)−N(43)	94(2)
Ag(1)−O(31)	2.59(5)	N(32P)−Pt(3)−N(43)	177(2)
Pt(1a)−Pt(3a)	7.678(4)	N(11)[a]−Ag(1)−N(1′2)	161(2)
Pt(1a)−Ag(1)	7.153(6)	N(11)[a]−Ag(1)−N(12)	104(2)
Ag(1)−Pt(3)	7.164(6)	N(1′2)−Ag(1)−N(12)	69(2)
Pt(2)−Ag(1)	7.189(5)	N(11)[a]−Ag(1)−N(1′1)[a]	68(2)
Ag(1)−Pt(2a)	7.225(6)	N(1′2)−Ag(1)−N(1′1)[a]	96(2)
Ag(1)−Pt(2)−Ag (1a)	88.2(1)	N(12)−Ag(1)−N(1′1)[a]	101.8(14)
Pt(2)−Ag(1)−Pt(2a)	91.8(1)	N(11)[a]−Ag(1)−O(32)	88(2)
Ag(1)−Pt(3)−Pt(1)	95.2(1)	N(1′2)−Ag(1)−O(32)	111(2)
Pt(3)−Pt(1)−Ag(1a)	103.5(1)	N(12)−Ag(1)−O(32)	115(2)
O(32)−Ag(1)−O(31)	47(2)	N(1′1)[a]−Ag(1)−O(32)	140(2)
		N(11)[a]−Ag(1)−O(31)	102(2)
		N(1′2)−Ag(1)−O(31)	91(2)
		N(12)−Ag(1)−O(31)	147(2)
		N(1′1)[a]−Ag(1)−O(31)	106(2)

[a] $1-x+2,-y+1,-z$.

Table 5. Experimental Data for the X-ray Diffraction Study of **8a** and Selected Bond Lengths (Å) and Angles (deg) of **8a**

(a) Experimental Data

formula	$C_{60}H_{128}O_{70}N_{52}Pt_6Ag_4$	volume (Å^3)	6536.9(22)
color, habit	yellow cubes	Z	2
crystal system	monoclinic	formula wt (g mol^{-1})	4300.16
space group	$P2_1/m$	temp (K)	123(2)
unit cell dimens	$a = 15.030(3)$ Å	final *R* indices (obs data)	$R_1 = 0.0801$; $wR_2 = 0.2023$
	$b = 22.002(4)$ Å, $\beta = 99.04(3)°$	*R* indices (all data)	$R_1 = 0.1235$; $wR_2 = 0.2513$
	$c = 20.016(4)$ Å	goodness-of-fit (obs data)	1.118

(b) Bond Lengths (Å) and Angles (deg) of **7**

Pt(1)−N(34′)	2.00(2)	N(34′)-Pt(1)−N(1)	88.7(7)	Ag(1)−N(11)	2.43(2)	N(11)−Ag(1)−N(11)[a]	96.6(10)
Pt(1)−N(14)	2.01(2)	N(14)−Pt(1)-N(12E)	174.8(8)	Ag(1)−N(11′)	2.47(2)	N(11)−Ag(1)-N(11′)	66.0(7)
Pt(1)−N(12E)	2.01(2)	N(14)−Pt(1)-N(11E)	94.2(8)	Ag(1)−O(41)	2.49(3)	N(11)[a]-Ag(1)−N(11′)	136.1(7)
Pt(1)−N(11E)	2.04(2)	N(12E)-Pt(1)−N(11E)	83.6(8)	Ag(2)−N(21)	2.39(2)	N(11′)−Ag(1)−N(11′)[a]	98.0(9)
Pt(2)−N(24)	1.98(2)	N(24)−Pt(2)-N(14′)	89.0(7)	Ag(2)−N(21′)	2.44(2)	N(21)−Ag(2)-N(21′)	68.2(6)
Pt(2)−N(14′)	2.04(2)	N(24′)-Pt(3)−N(34)	90.9(8)	Ag(2)−O(61)	2.51(4)	N(31′)−Ag(3)−N(31)	67.4(6)
Pt(3)−N(24′)	2.03(2)			Ag(3)−N(31′)	2.41(2)	O(52)−Ag(4)-O(102)	137(2)
Pt(3)−N(34)	2.04(2)			Ag(3)−O(63)[b]	2.44(4)	O(52)−Ag(4)-O(111)	94.7(14)
Pt(1)−Pt(2)	7.841(2)			Ag(3)−N(31)	2.47(2)	O(102)−Ag(4)-O(111)	127(2)
Pt(1)−Pt(3)	7.712(3)			Ag(3)−N(31)[a]	2.47(2)		
Pt(2)−Pt(3)	7.784(2)			Ag(4)−Ag(4)[a]	1.31(2)		

[a] $x,-y+1/2,z$. [b] $x-1,y,z$.

roughly equilateral (9.62 Å, av). The three sets of Pt_3 and Ag_3 triangles are close to parallel with distances of 5.24 Å between Pt_3 and Ag_3 and 10.48 Å between the two Pt_3 triangles.

There are several structural details of **8a** which are of interest. First, the central cavity hosts a silver cation and in addition three nitrate anions. The Ag^+ ion is disordered over two positions at either side of the mirror plane (deviation from plane is 0.65(1) Å), and three nitrate anions, with their planes perpendicular to the central Ag_3 plane, bind to the disordered Ag^+. Second, there are two additional NO_3^- ions, one at either

end of the barrel. These NO_3^- ions are close to the Pt triangles, yet not in the plane of these. Rather Pt_3 and NO_3^- planes form an angle of 49(2)° with one of the nitrate oxygen atoms pointing toward the disordered Ag^+ in the central cavity (O(23)−Ag(4), 3.92(5) Å). Thus altogether five NO_3^- ions are associated with the cation of **8a** to reduce the high positive charge of +16. In the crystal lattice, adjacent cations of **8a** are bridged by a NO_3^- anion, which (semi-) chelates both Ag(2) (Ag(2)−O(61), 2.51(4) Å; Ag(2)−O(62), 2.63(4) Å) and Ag(3) of the symmetry related cation ($x+1,y,z$; Ag(3)−O(62), 2.65(4) Å; Ag(3)−O(63), 2.44(4) Å). In this way cations of **8a** are arranged along the *x*-axis like beads on a string. The centers of these beads are 15 Å apart, but the closest intermetallic distance, between the NO_3^- bridged Ag(2) and Ag(3) sites, is 5.273(5) Å. The second cation **8a** within the unit cell is part of another string of beads which runs antiparallel to the former. Two strings are approximately 16 Å apart (center to center of cations **8**). NO_3^- anions not associated with the complex cations as well as water molecules fill the space between the strings and are multiply interconnected through H bonds.

Conclusions

Complex formation of enPt^{II} with 2,2′-bipyrazine (bpz) leads in a kinetically controlled reaction and in reasonable yield to a cyclic trimer of composition $[\{enPt(bpz\text{-}N4,N4')\}_3]^{6+}$, **1**. Due to the low barrier of rotation about the central C2−C2′ bond of the bpz ligand and because of monodentate binding of each pyrazine half to the heavy metal, the molecular triangle **1** is rather flexible. This feature makes **1** different from other triangles with spatially fixed donor sites at the bridging ligands which do not permit large torsional variations.[14,16,23] **1** has been crystallized in two distinctly different forms, with an all-trans orientation of the two pyrazine entities (C_2 molecular symmetry) and an all-cis arrangement of the pyrazine rings (approximately C_3 symmetry). There is indirect evidence from low-temperature solution NMR studies that intermediates between these two forms exist. In compound **1b**, all-cis and all-trans forms crystallize side by side. The two forms differ markedly in intermetallic distances. **1** is of interest for several reasons. First, in its all-cis form it behaves as an efficient ligand toward additional metal electrophiles such as enPt^{II}, enPd^{II}, and Ag^+, affording highly charged multinuclear species of different topologies, with vases, a paddle wheel, and a barrel crystallographically characterized. Second, both kinds of triangles and the higher nuclearity derivatives of the all-cis conformer display pronounced affinities for anions, hence act as positively charged anion receptors.[35] Receptor specificity appears to depend on the shape and dimensions of the cavity provided by the Pt triangle, although the anion by itself may play an active role in switching one conformer into another. This latter possibility is ruled out in the hexanuclear vases, however. The anion binding pattern is particularly interesting with the all-cis conformer of **1** in that it either incorporates two *different* anions simultaneously, NO_3^- and ClO_4^-, or a single PF_6^- only. The feature of simultaneous binding of two different anions, NO_3^- and PF_6^-, is also seen with the hexanuclear vases **3**−**6**. Third, the container complex **8a**, an inorganic version of a carceplex, has both a cation (Ag^+) and anions (NO_3^-) incorporated in the interior. Fourth, the kinetic product **1** can be cleanly converted into its thermodynamic product, which is the chelate $[enPt(bpz\text{-}N1,N1')]^{2+}$ (**2a**). Although the synthetic potential of **2a** has not yet been explored by us, it is feasible that it functions as a similar building block as $[enPd(bpz\text{-}N1, N1')]^{2+}$ (**2**), which is the starting material for another type of molecular triangles,[30] containing metal ions at the corners and at the centers of the sides.

Experimental Section

Preparations. $enPdCl_2$,[36] $enPtCl_2$,[37] and pz[38] were prepared according to the references. Compound $[\{enPt(bpz\text{-}N4,N4')\}_3](NO_3)_6$ (**1**) was prepared in a slightly modified version (2 d, 80 °C) of that previously reported in ref 20, now in yields of 65%. The preparation of **2** is also given in ref 20. The pure nitrate compound $[enPd(bpz\text{-}N1,N1')](NO_3)_2$ (**2***) was prepared in a manner analogous to **2** in solution except for the addition of $NaClO_4$. The hexanuclear Pt_3Pd_3 complex **3** (mixed NO_3^-, PF_6^- salt) and its pure NO_3^- salt **3*** were prepared as described in ref 21.

We note that due to rapid loss of water of crystallization, elemental analysis data of the compounds described below frequently indicated a lower water content than was established by X-ray analysis.

$[\{enPt(bpz\text{-}N4,N4')\}_3](NO_3)_2(ClO_4)_4\cdot H_2O$ (1a) and $[\{enPt(bpz\text{-}N4,N4')\}_3](NO_3)_2(PF_6)_4\cdot 5.25H_2O$ (1b). The trinuclear compound **1** (100 mg, 0.058 mmol) was dissolved in water (10 mL). After addition of 4 equiv of $NaClO_4$ (NH_4PF_6) the mixture was concentrated to 5 mL under vacuum and filtered. Colorless crystals of **1a** (**1b**) were isolated in 82% (85%) yield after 7 days at 4 °C. Elemental analysis for the dihydrate of **1a** ($Pt_3N_{20}C_{30}Cl_4H_{46}O_{24}$): Anal. Calcd: C, 20.0; H, 2.6; N, 15.6. Found: C, 20.0; H, 2.5; N, 15.6. Monohydrate of **1b** ($Pt_3N_{20}C_{30}P_4F_{24}H_{44}O_7$): Anal. Calcd: C, 18.3; H, 2.3; N, 14.3. Found: C, 18.0; H, 2.7; N, 14.6.

$[enPt(bpz\text{-}N1,N1')](NO_3)_2$ (2a). The kinetic reaction product **2** converts into the thermodynamic product **2a** during heating of a solution (H_2O) of **2** for 14 days at 100 °C. Elemental analysis for **2a** ($PtN_8C_{10}H_{14}O_6$): Anal. Calcd: C, 22.4; H, 2.6; N, 20.9. Found: C, 22.4; H, 2.6; N, 20.9. ^{1}H NMR (200 MHz, D_2O, TSP): δ 2.95 (s, 8H; CH_2), 8.89 (d, $^3J_{5,6} = 3.3$ Hz, 2H; arom.), 9.08 (d, $^3J_{5,6} = 3.3$ Hz, 2H; arom.), 9.81 (d, 1 Hz, 2H; arom.). ^{195}Pt NMR (43 MHz, D_2O): δ −2749 (PtN_4).

$[\{enPt(N4,N4'\text{-}bpz\text{-}N1,N1')Pten\}_3](NO_3)_7(PF_6)_5\cdot 4H_2O$ (4). $enPtCl_2$ (56.9 mg, 0.174 mmol) was suspended in water (10 mL) and stirred for 1 h at 80 °C with $AgNO_3$ (56.3 mg, 0.311 mmol). After removal of AgCl by filtration and addition of **1** (100 mg, 0.058 mmol) to the filtrate, the mixture was stirred for 3 days at 80 °C. The orange reaction mixture was filtered and NH_4PF_6 (75 mg, 0.460 mmol) was added. Yellow-orange crystals of **4** were isolated in 23% yield after 7 days at 4 °C. Elemental analysis for the anhydrous form of **4** ($Pt_6N_{31}C_{36}H_{66}O_{21}P_5F_{30}$): Anal. Calcd: C, 13.7; H, 2.1; N, 13.7. Found: C,13.6; H, 2.6; N, 13.7. ^{1}H NMR (200 MHz, D_2O, TSP): δ 2.7 (s, 8H; CH_2), 9.26 (d, $^3J_{5,6} = 3.9$ Hz, 2H; arom.), 9.81 (d, $^3J_{5,6} = 3.9$ Hz, 2H; arom.), 10.56 (s, 2H; arom.).^{195}Pt NMR (43 MHz, D_2O): δ −2704 and −2715 (PtN_4).

$[\{enPd(N4,N4'\text{-}bpz\text{-}N1,N1')Pden\}_3](NO_3)_4(PF_6)_8\cdot 5H_2O$ (5). $enPdCl_2$ (100 mg, 0.421 mmol) was suspended in water (10 mL) and stirred for 3 h at room temperature with $AgNO_3$ (136 mg, 0.801 mmol). After removal of AgCl by filtration and addition of **2*** (0.400 mmol) to the filtrate, the mixture was stirred for 1 day at room temperature. The orange reaction mixture was filtered and NH_4PF_6 (250 mg, 1.5 mmol) was added. Yellow-orange crystals of **5** were isolated in 83% yield after 5 days at 4 °C. Elemental analysis for the anhydrous form of **5** ($Pd_6N_{28}C_{36}H_{66}O_{12}P_8F_{48}$): Anal. Calcd: C, 15.0; H, 2.3; N,13.6. Found: C, 15.0; H, 2.4; N, 13.6.

$[\{enPd(N4,N4'\text{-}bpz\text{-}N1,N1')Pten\}_3](NO_3)_7(PF_6)_5\cdot 9.75H_2O$ (**6**) was prepared by combining an aqueous solution of the mononuclear **2a** with 1 equiv of $[enPd(H_2O)_2]^{2+}$ which had been prepared from $enPdCl_2$ in the same manner as described above. The orange reaction mixture was stirred for 1 day at room temperature and filtered and NH_4PF_6 (8 equiv) was added. Yellow-orange crystals of **6** were isolated in 81% yield after 5 days at 4 °C. Elemental analysis for the hexahydrate form of **6** ($Pt_3Pd_3N_{31}C_{36}H_{78}O_{27}P_5F_{30}$): Anal. Calcd: C, 14.4; H, 2.6; N, 14.4. Found: C, 14.3; H, 2.7; N, 14.4.

(35) Schmidtchen, F. P.; Berger, M. *Chem. Rev.* **1997**, *97*, 1609 and references cited therein.

(36) Dhara, S. C. *Indian J. Chem.* **1970**, *8*, 193.

(37) Kauffman, G. B.; Cowan, D. O. *Inorg. Synth.* **1963**, *7*, 239.

(38) Crutchley, R. J.; Lever, A. B. P. *Inorg. Chem.* **1982**, *21*, 2276.

[{enPt(bpz-N4,N4′)}$_3$AgNO$_3$]$_2$(NO$_3$)$_8$(PF$_6$)$_4$·15.5H$_2$O (7). 2 (100 mg 0.058 mmol) was dissolved in water (5 mL) then $AgPF_6$ (14.7 mg, 0.058 mmol) was added with stirring for 1 day. After filtration yellow crystals of **7** were isolated in 50% yield after 3 days at 4 °C. Elemental analysis for **7** ($Pt_6Ag_2N_{46}C_{30}H_{115}O_{45.5}P_4F_{24}$): Anal. Calcd: C, 17.3; H, 2.8; N, 15.5. Found: C, 17.4; H, 2.7; N, 15.3.

[{enPt(bpz-N4,N4′)}$_3$AgNO$_3$]$_3$(NO$_3$)$_{12}$·AgNO$_3$·22H$_2$O (8a). 2 (100 mg 0.058 mmol) and $AgNO_3$ (0.198 mg, 0.116 mmol) were dissolved in 5 mL of water and stirred for 1 day at room temperature. **8a** was isolated as yellow crystals in 90% yield after 7 days at 4 °C. Elemental analysis for the tetrahydrate form of **8a** ($Pt_6Ag_4N_{52}C_{60}H_{92}O_{52}$): Anal. Calcd: C, 18.1; H, 2.3; N, 18.3. Found: C, 18.2; H, 2.4; N, 18.2.

Association Constants. The ^{1}H NMR spectra were measured at constant temperature (20 °C) and constant pD (2.9). The various salts (NH_4PF_6, $NaClO_4$, $NaBF_4$, Na_2SO_4) were added to the pure nitrate salt of **1** and **3*,** respectively (0.01 mol/L), with increasing concentrations (1 to 10 equiv). Three independent measurements were performed for each salt and changes in chemical shifts of individual bpz resonances were monitored in a similar way as previously reported for **3***.[21] The association constants (K_{ass}) were determined according to ref 39 with a nonlinear least-squares method. The individual results did not differ from each other within the error limits. K_{ass} (standard deviation 3σ) is the weighted mean of the results of the three independent measurements.

Instrumentation. ^{1}H NMR spectra were recorded at 20 °C on a Bruker AC 200 FT NMR spectrometer in D_2O (with TSP as internal standard) or DMF-d_7, respectively. Elemental analyses were performed with a Carlo Erba Model 1106 Strumentazione Element-Analyzer.

X-ray Crystal Structure Determinations. Intensity data for **1a**, **1b**, **2a**, **4**, **5**, **6**, **7**, and **8a** were collected on an Enraf-Nonius KappaCCD[40] (Mo Kα, $\lambda = 0.71069$ Å, graphite-monochromator) with sample-to-detector distances of 28.7 (**5**), 30.2 (**2a**), 30.7 (**4**), 32.7 (**8a**), 34.7 (**1a**), and 35.7 mm (**1b**, **6**, **7**), respectively. They covered the whole sphere of reciprocal space by measurement of 360 (1061 for **1b**) frames rotating about ω in steps of 1°. The exposure times were 20 (**2a**), 30 (**6**), 40 (**1a**, **1b**), 45 (**4**), 50 (**7**, **8a**), and 60 s (**5**) per frame. Preliminary orientation matrices and unit cell parameters were obtained from the peaks of the first 10 frames, respectively, and refined using the whole data set. Frames were integrated and corrected for Lorentz and polarization effects using DENZO.[41] The scaling as well as the global refinement of crystal parameters were performed by SCALEPACK.[41] Reflections, which were partly measured on previous and following frames, are used to scale these frames on each other. Merging of redundant reflections in part eliminates absorption effects and also considers a crystal decay if present.

The structures were solved by standard Patterson methods[42] and refined by full-matrix least-squares based on F^2 using the SHELXTL-PLUS[43] and SHELXL-93 programs.[44] The scattering factors for the atoms were those given in the SHELXTL-PLUS program. Transmission factors were calculated with SHELXL-97.[45] Hydrogen atoms were included in calculated positions and refined with isotropic displacement parameters according to the riding model, except for the aliphatic hydrogen atoms of the ethylenediamine in **4**, which were not further refined. Part of the anions and water molecules in all structures are disordered.

Acknowledgment. This work has been supported by the Deutsche Forschungsgemeinschaft and the Fonds der Chemischen Industrie. We dedicate this paper to Prof. Dr. Dirk Walther, University of Jena, on the occasion of this 60th birthday.

Supporting Information Available: ^{1}H NMR spectra (**1**; **1** + salts; interconversion **1** → **2**; comparison of **1**, **2a**, **3***, and **4**), views of cations **2a**, **4**, **5**, and **6**, tables of crystal data, structure solution and refinement, atomic coordinates, anisotropic thermal parameters, bond distances and angles for compounds **1a**, **1b**, **2a**, **4**, **5**, **6**, **7**, and **8a** (PDF). This material is available free of charge via the Internet at http://pubs.acs.org.

JA9931325

(39) Sigel, H.; Scheller, K. H.; Rheinberger, V. M.; Fischer, B. E. *J. Chem. Soc., Dalton Trans.* **1980**, 1022.
(40) NONIUS BV, KappaCCD package, Röntgenweg 1, P.O. Box 811, 2600 AV Delft, The Netherlands.
(41) Otwinowsky, Z.; Minor, W. *Methods Enzymol.* **1996**, *276*, 307.
(42) Sheldrick, G. M. *Acta Crystallogr. Sect. A* **1990**, *A46*, 467.
(43) Sheldrick, G. M. SHELXTL-PLUS (VMS), Siemens Analytical X-ray Instruments, Inc.: Madison, WI, 1990.
(44) Sheldrick, G. M. SHELXL-93, Program for crystal structure refinement, University of Göttingen, Germany, 1993.
(45) Sheldrick, G. M. SHELXL97, Program for the Refinement of Crystal Structures, University of Göttingen, Germany, 1997.